(DRAFT) Preliminary study of lava flow morphology, chemistry, and distribution on the Alarcon Rise, Gulf of California, Mexico

Patricia Lieberg-Clark, Cabrillo College

Mentors: David Clague, Julie Martin, Jenny Paduan, and Ryan Portner

Summer 2012

Keywords: submarine volcanism, mid-oceanic ridge processes, seafloor morphology, magma viscosity

ABSTRACT

The Alarcon Rise is a northern component of the East Pacific Rise, located at the aperture of the Gulf of California at a depth of approximately 2400 meters. MBARI's Submarine Volcanism Lab and Mapping AUV Team surveyed the ridge in the spring of 2012. During these surveys, the teams created high-resolution maps and collected rock and sediment samples of the ~50-km neovolcanic zone and off-axis seamount to the northwest of the Rise. Clague subsequently performed geochemical analyses of the Alarcon glass samples, while crystal analysis was performed as a component of this summer intern project. Geochemical and crystallinity data were utilized to determine the magma viscosities of rock samples collected on the Alarcon Rise in 2003 and 2012. These magma viscosity data were then correlated to each sample's respective lava flow morphology: pillow, sheet or lobate. We propose that sea floor morphology on the Alarcon Rise is determined primarily by the viscosity of the magma that formed the flow.

INTRODUCTION

The Earth's divergent plate boundaries are mid-oceanic ridges (MORs) that comprise the longest mountain range on the planet, forming a series of mostly continuous chains with a combined length of more than 80,000 km. These submarine mountain ranges are sites of sea floor spreading, as they are composed of enumerable volcanoes that emplace a variety of lava flow types within the neovolcanic zone and vicinity.

MORs produce several types of lava that are generally classified by their morphology. The three main designations of lava morphologies include: pillow, sheet, and lobate flows (Figure 1). Pillow lavas are bulbous in form, sheets are flat and wide, while lobate flows are broad, flattened pillows, manifesting attributes of the both pillow and sheet morphologies.

Pillow Flow Lobate Flow Sheet Flow

Figure 1. The three primary morphologies of submarine lava.

Studies show that the different flow morphologies are dictated by the flow's respective eruption rate (Clague and Paduan 2008 ADD 1). Analog experiments with wax have also shown that submarine lava morphologies are determined by the eruption rates of the magma for which they are composed (Figure 2 and 3). Slow eruption rates yield pillow lavas, fast rates yield sheet flows, and lobate flows are transitional between pillow and sheet. Pillows lavas tend to form when the crustal flow rate exceeds the effusion rate, and this type of flow transitions to lobates, then sheets, when crustal flow rate decreases, and/or effusion rate increases (Gregg and Fink 1995, Clague and Paduan 2008, ADD 1).

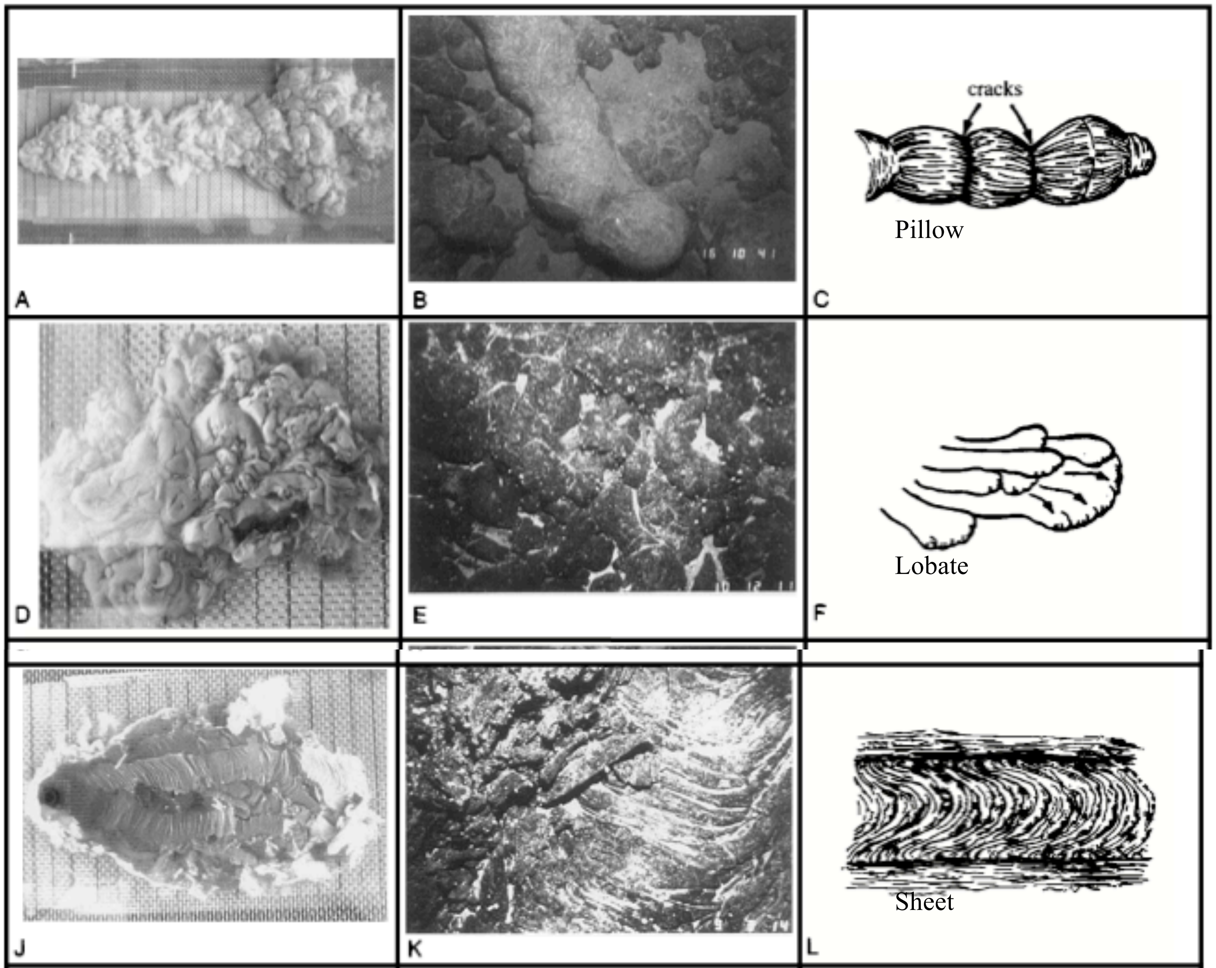

Figure 2. Results of flow experiments with wax. The left-hand panel in each row is a photograph of the wax analog of one of three main lava flow regimes (pillow, lobate, or sheet). The middle panel in each row is a photograph of the relevant seafloor morphology in nature, and the third panel is an illustration of the relevant flow morphology (Adapted from Gregg and Fink, 1995).

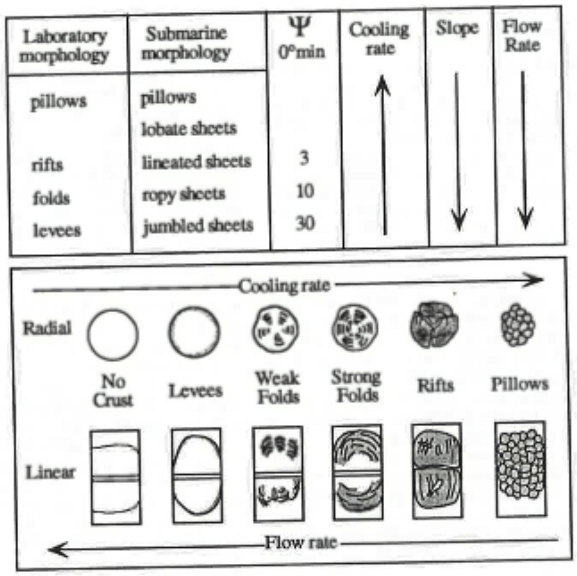

Figure 3. (a.) Correlation between wax morphologies derived in the laboratory, and submarine lava morphologies. The laboratory-derived relationship incorporates the effects of convection, heat capacity, thermal diffusivity, and density of the flow. (b.) Illustrations of morphological flow types developed for increasing cooling/eruption rates pertaining to the upper (radial) and lower (linear) geometry in analog experiments (Griffiths and Fink 1992; Gregg and Fink 1995).

The eruption rate is controlled by an interplay between three factors: dike intrusion width, gas content, and viscosity of the magma. Dike intrusion width is virtually impossible to quantify, as is an accurate measurement of gas content. Magma viscosity, on the other hand, is an eruption rate parameter that is quantifiable with rock and glass samples from the sea floor. Magma viscosity may be calculated with a formula that incorporates the melt viscosity and the crystallinity of the rock.

The three lava flow types: pillow, lobate, and sheet, have a tendency to form at different types of sea floor spreading centers (Perfit and Chadwick 1998). Pillow lavas tend to be found predominantly on ridges that have relatively slow sea floor spreading rates, such as the Mid-Atlantic Ridge (~20 mm/year). Sheet flows, on the other hand, are generally observed at fast spreading centers, such as the East Pacific Rise (~110 mm/year).

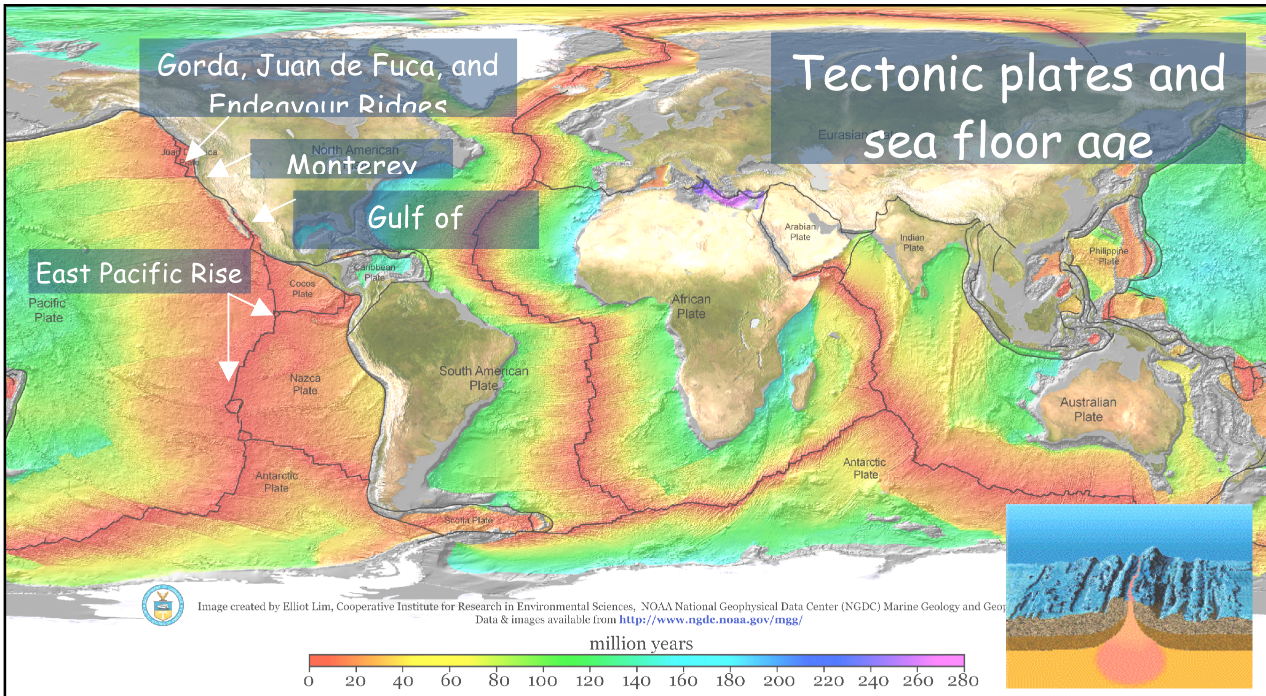

Figure 4. Lithospheric plate boundaries depicted with sea floor age.

Ridge systems that are considered intermediate-rate spreading centers (~4-8 cm/year) are comprised of all three of the lava morphologies: pillow, sheet, and lobate. The Alarcon Rise in the southern Gulf of California is such an intermediate sea floor spreading center with a spreading rate of approximately 4.8 cm/year. Pillow, sheet, and lobate flow morphologies form on the Alarcon Rise, making this ridge system an ideal location to analyze the effect of viscosity on flow morphology.

The Gulf of California Expeditions – Data from the Alarcon Rise

In 2003 and the spring of 2012, David Clague and his team from MBARI's submarine volcanism lab conducted surveys of the lava flows that comprise the Alarcon Rise at the southern end of the Gulf of California between Cabo San Lucas and the Mexican mainland. The studies were conducted as a part of MBARI's larger expeditions to the Gulf of California (Figure 6). In the spring of 2012, Clague's team utilized the RV Western Flyer and the *ROV Doc Ricketts* and a research sled that was designed to collect rock and glass samples, push cores, and video of the submarine topography (Figure 7). They also utilized the high-resolution maps created by MBARI's Mapping AUV Team from the *RV Zephyr*. The objective of this summer internship project was to identify lava flow morphologies and distribution on the Alarcon Rise.

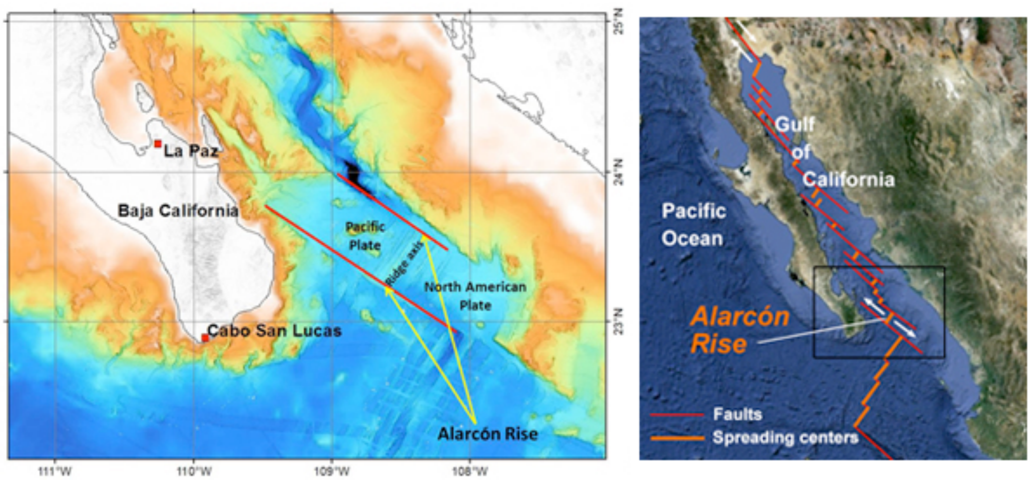

Figure 5. The southern Gulf of California, Mexico, and the location of the Alarcon Rise.

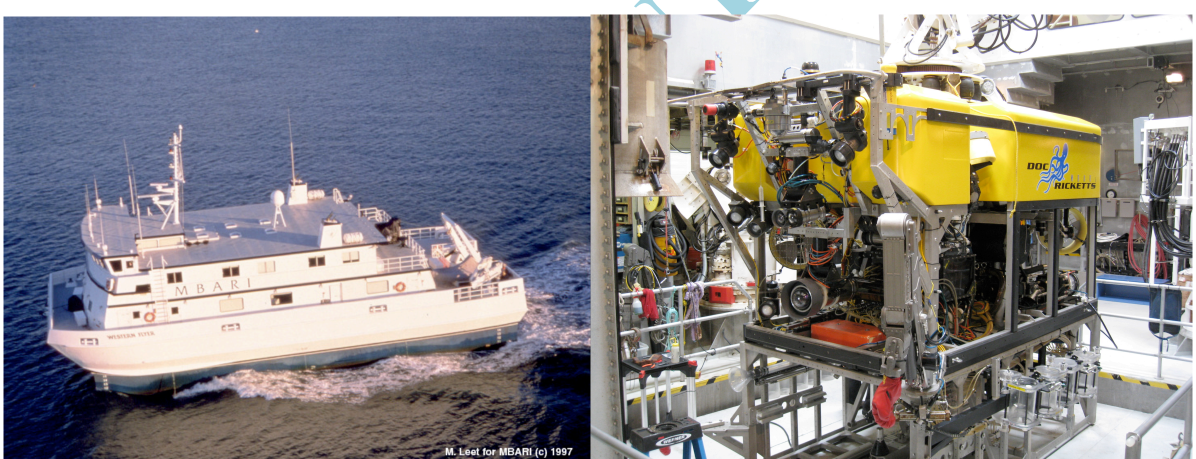

Figure 6. The *RV Western Flyer* and the *ROV Doc Ricketts.*

MATERIALS AND METHODS

I.) Identify lava flow morphologies & distribution:

A.) ArcMap (V. 10.0) was used to import and map rock and glass sample geochemistry, rock crystal fraction data, and confirmed lava morphology on high-resolution maps created with the bathymetric data collected by the *AUV D. Allan B.*

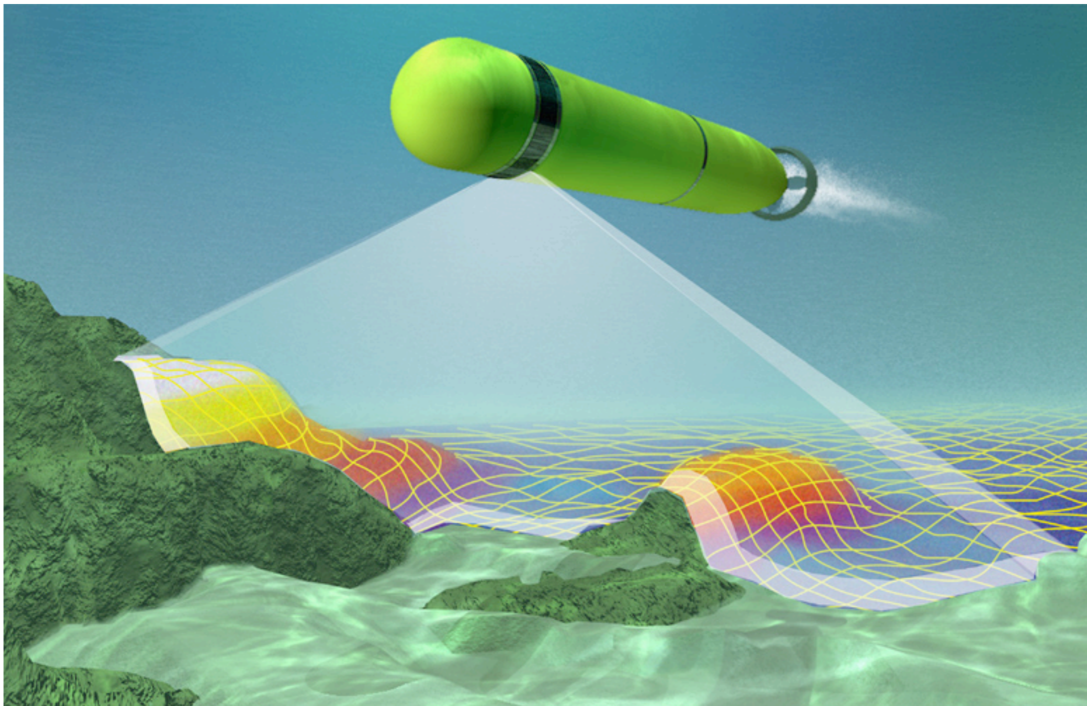

Figure 7. The *AUV D. Allan B.*

B.) Confirmation of lava flow type via observations through video from the ROV Doc Ricketts

The idea was to eventually end up with a high-resolution map that depicted accurate borders around each individual lava flow on the Alarcon Rise.

Figure 8. Video Lab Station at MBARI

The designations of the individual lava flows would be determined by:

1. High-resolution AUV maps and GIS: Allow us to study the seafloor physiography of the Rise. Appropriate color-ramping techniques would be utilized to emphasize these changes in bottom topography.
2. Glass chemistry: Dr. Clague's microprobe analyses of the Alarcon glass samples provided valuable insight into the chemistry of the parent melt. MgO, in particular provides a signature for a given melt, and can be very useful when attempting to identify individual lava flows. Dr. Clague is presently conducting analyses of the ages of the Alarcon lava flows, which will give the team additional confirmation of individual flow designations.

II.) Crystal fraction Analysis

The magma viscosity calculation requires the major element glass chemistry, melt temperature and crystal fraction of the magma. The melt temperatures were derived from the normalized % MgO in the glass samples for each collection site. Glass chemistries were determined through microprobe analysis performed by Dr. Clague, at the University of California at Davis.

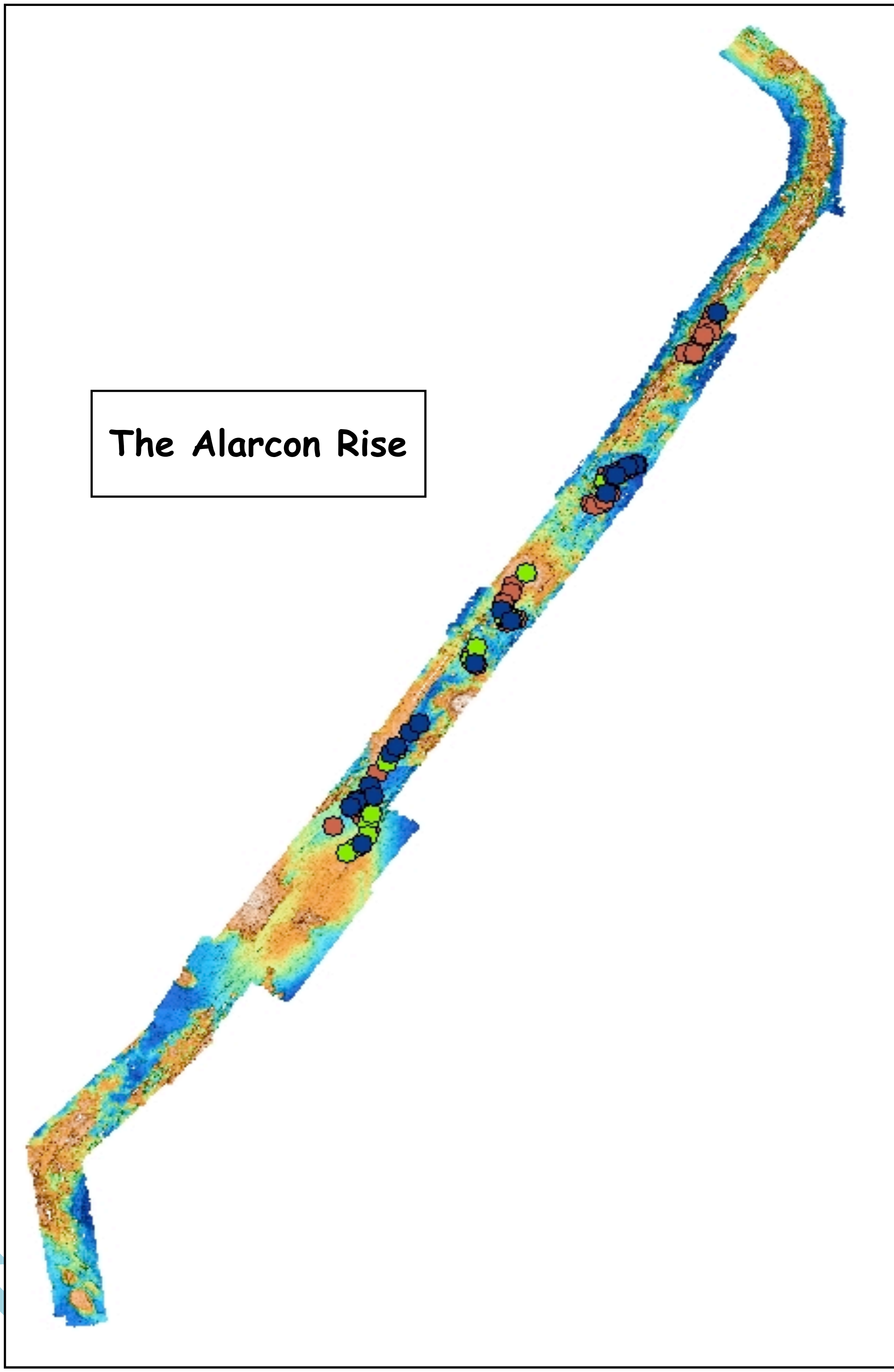

Figure 9. High-resolution map This is a map of the high-resolution AUV bathymetric data, showing the full extent of the Alarcon Rise in the Gulf of California. The length of the axial ridge (distance from bend to bend) is approximately 50 km.

A compound microscope (Leica MZ 12) was used to estimate the percentage of crystals (phenocrysts) in ~80 crushed rock samples collected by the *ROV Doc Ricketts***.**

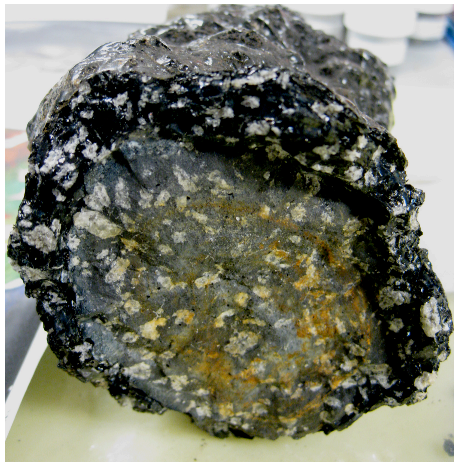

Figure 10. Fresh surface of a plag-phyric pillow lava on the Alarcon Rise.

Figure 11. (a.) Plag-phyric pillow bud from the sea floor on the Alarcon Rise. (b.) The Leica microscope used in the crystal analysis in the Clague lab. (c.) View of plagioclase phenocryst under the compound microscope.

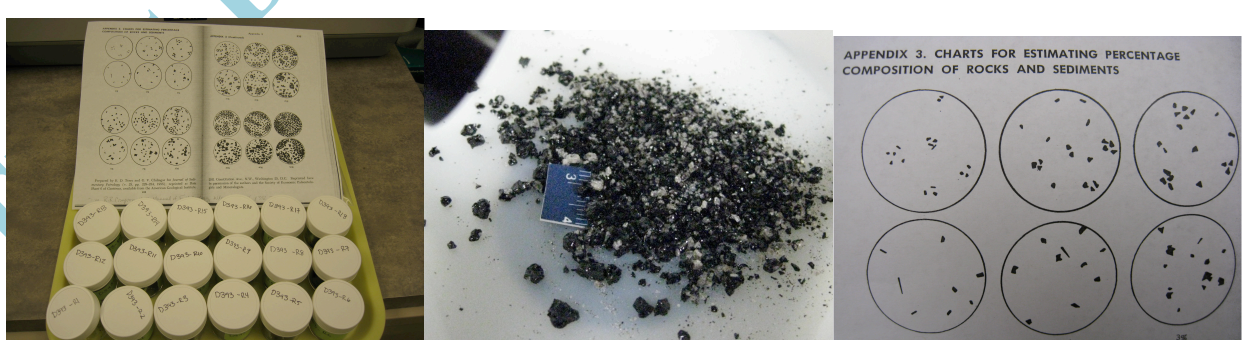

Figure 12. (a.) Tray with jars of crushed rock samples and Composition Percentage Estimation Chart. These samples were collected by the *ROV Doc Ricketts* in the spring of 2012. (b.) Weighing boat with crushed rock sample from the Alarcon Rise. (c.) Composition Percentage Estimation Chart (Compton 1962),

RESULTS

I.) Identification of lava flow morphologies & distribution:

A.) The Mapping AUV data collected via the D. Allan B, was digitized and incorporated into shapfiles for ArcMap (V. 10.0). The Doc Ricketts ROV tract was also added to the map files, as were the rock sample collection locations. We then confirmed the lava flow morphology via observations through video collected with the *ROV Doc Ricketts*.

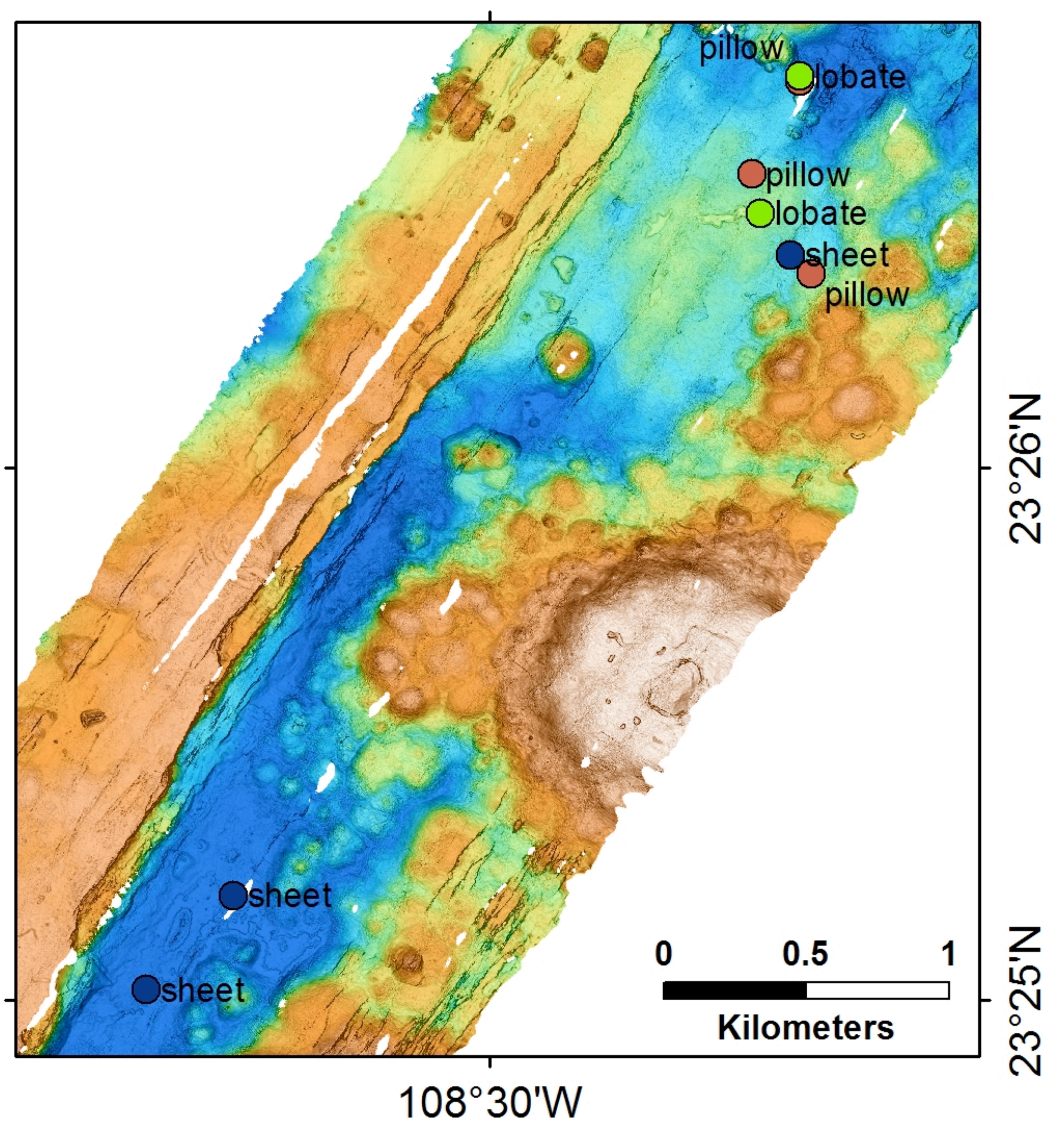

Figure 13. Close-up view of the Alarcon Rise. AUV bathymetry data is gridded at 1m resolution. The blue regions show the greatest depth, while the orange-to-brown regions illustrate the shallower depths, accentuating the elevated topography created by the individual lava flows. The colored dots represent confirmed lava flow morphologies of rock samples collection by the *ROV Doc Ricketts* in the spring of 2012. This figure depicts a small excerpt of GIS mapping work for the Alarcon Rise that is in progress. The lava flow boundaries have yet to be depicted on the image.

B.) Confirmation of lava flow relationships through microprobe analysis.

Table 2. Excerpt of an Excel spreadsheet depicting some results of microprobe analysis for glass samples from the Alarcon Rise collected in 2012. The MgO data are normalized and displayed with corresponding temperature data.

Alarcon Rise	SiO2	TiO2	Al2O3	FeO	MnO	MgO	MgO*1.05	CaO	Na2O	K2O	P2O5	S	Cl	Total	New Total	
D394-R18 avg	50.62	1.48	15.54	9.88	0.17	7.61	7.99	12.02	2.76	0.14	0.15	0.123	0.007	100.51	100.89	0.991210933
D394-R19 avg	50.45	1.58	15.73	9.73	0.18	7.53	7.91	11.92	2.85	0.17	0.16	0.118	0.014	100.42	100.80	0.992097349
D394-R20 avg	50.70	1.69	15.18	10.43	0.16	7.31	7.68	11.62	2.92	0.16	0.18	0.137	0.013	100.51	100.87	0.991344374
D394-R21 avg	50.37	1.86	15.05	10.92	0.18	6.89	7.23	11.20	2.99	0.19	0.18	0.146	0.022	100.00	100.34	0.996603078
D394-R22 avg	50.33	1.49	15.62	10.07	0.20	7.55	7.93	11.84	2.78	0.14	0.17	0.126	0.005	100.32	100.69	0.99310793
D394-R23 avg	49.85	1.37	16.38	9.26	0.18	8.16	8.57	12.22	2.79	0.09	0.13	0.113	0.013	100.55	100.96	0.990496091
D395-R01 avg	50.00	1.38	16.17	9.44	0.16	8.00	8.40	12.22	2.84	0.10	0.13	0.134	0.004	100.56	100.96	0.990451454
D395-R02 avg	50.42	1.97	15.12	11.21	0.18	6.84	7.18	10.95	3.07	0.21	0.22	0.156	0.023	100.38	100.72	0.992863003
D395-R08 avg	50.34	1.97	15.08	11.21	0.19	6.79	7.13	10.99	3.03	0.20	0.22	0.132	0.021	100.18	100.52	0.994820962
D395-R09 avg	50.63	2.00	14.95	11.19	0.21	6.73	7.07	11.04	3.08	0.19	0.22	0.143	0.029	100.41	100.74	0.992640169
D395-R10 avg	50.43	1.29	16.34	9.12	0.18	8.14	8.54	12.25	2.72	0.14	0.13	0.112	0.000	100.84	101.25	0.987687585
D395-R11 avg	50.42	1.29	16.37	9.03	0.16	8.17	8.58	12.39	2.69	0.14	0.14	0.104	0.007	100.92	101.33	0.986898722
D395-R12 avg	50.36	1.52	15.73	9.81	0.16	7.61	7.99	12.03	2.85	0.16	0.17	0.128	0.010	100.54	100.92	0.990924617
D395-R13 avg	50.20	1.51	15.83	9.63	0.15	7.78	8.17	11.88	2.83	0.15	0.17	0.118	0.003	100.26	100.65	0.993527467
D395-R14 avg	50.56	2.01	15.02	11.21	0.20	6.68	7.01	10.92	3.10	0.20	0.23	0.137	0.028	100.30	100.64	0.993681379
D395-R17 avg	50.46	1.97	15.03	11.31	0.19	6.87	7.21	10.91	3.05	0.19	0.21	0.144	0.019	100.36	100.71	0.992992354
D395-R20 avg	50.48	1.97	15.15	11.12	0.18	6.81	7.16	11.03	3.09	0.19	0.21	0.142	0.023	100.40	100.75	0.992599969
D395-R22 avg	50.63	1.95	15.05	11.19	0.17	6.82	7.16	10.99	3.08	0.21	0.23	0.139	0.025	100.47	100.81	0.991954259
D395-R23 avg	50.47	1.99	15.05	11.21	0.19	6.74	7.08	10.96	3.09	0.21	0.22	0.148	0.027	100.30	100.63	0.993718605
D395-R31 avg	50.61	2.00	15.09	11.25	0.19	6.84	7.19	10.99	3.07	0.19	0.21	0.143	0.027	100.62	100.96	0.990495699
D396-R01 avg	50.80	1.69	15.03	10.38	0.17	7.18	7.54	11.84	2.95	0.17	0.16	0.116	0.017	100.51	100.87	0.991393416
D396-R02 avg	50.88	2.01	14.78	11.47	0.19	6.39	6.71	10.71	3.21	0.25	0.27	0.143	0.011	100.30	100.62	0.993802449
D396-R03 avg	50.41	1.39	15.93	9.36	0.18	7.87	8.27	12.24	2.79	0.13	0.15	0.118	0.001	100.58	100.97	0.990373765
D396-R04 avg	50.64	1.44	15.91	9.56	0.17	7.86	8.25	12.15	2.83	0.13	0.16	0.118	0.008	100.96	101.35	0.986654122
D396-R05 avg	50.85	1.68	14.99	10.54	0.16	7.24	7.60	11.89	2.94	0.16	0.16	0.149	0.009	100.77	101.13	0.988854424
D396-R06 avg	50.69	2.04	14.71	11.52	0.19	6.38	6.70	10.83	3.18	0.22	0.25	0.137	0.025	100.17	100.49	0.995094087
D396-R07 avg	51.67	2.15	14.39	12.08	0.22	5.38	5.65	9.82	3.51	0.34	0.35	0.135	0.031	100.08	100.35	0.996528394
D396-R08 avg	52.59	2.59	13.42	13.76	0.26	4.07	4.27	8.25	3.73	0.47	0.49	0.155	0.067	99.84	100.04	0.999570684
D396-R09 avg	50.88	1.60	15.08	10.21	0.17	7.36	7.73	12.07	2.93	0.16	0.16	0.121	0.011	100.74	101.11	0.989044649
D396-R10 avg	50.78	1.77	14.88	10.82	0.19	6.82	7.16	11.51	3.11	0.18	0.18	0.134	0.011	100.39	100.73	0.992788681
D396-R11 avg	51.44	2.12	14.27	12.08	0.22	5.61	5.89	9.93	3.43	0.30	0.34	0.137	0.030	99.92	100.20	0.99800708
D396-R12 avg	50.80	1.55	14.88	10.29	0.18	7.23	7.59	12.08	2.91	0.12	0.16	0.146	0.004	100.34	100.70	0.993004482
D396-R13 avg	50.81	1.61	15.05	10.31	0.18	7.20	7.56	12.07	2.95	0.15	0.17	0.127	0.014	100.65	101.01	0.989959729
D396-R14 avg	50.74	1.87	14.80	10.99	0.20	6.88	7.22	11.36	3.09	0.18	0.16	0.141	0.015	100.41	100.75	0.992565782
D396-R15 avg	50.46	1.48	15.54	9.75	0.16	7.61	7.99	12.13	2.86	0.15	0.15	0.125	0.006	100.43	100.81	0.992007396
D396-R16 avg	51.11	2.07	14.22	11.83	0.20	5.98	6.28	10.68	3.33	0.28	0.25	0.154	0.036	100.14	100.44	0.995601829
D396-R17 avg	50.57	2.10	14.91	11.64	0.20	6.54	6.87	10.82	3.18	0.22	0.24	0.133	0.026	100.57	100.89	0.991147369

C.) Crystal Fraction Analysis (Determination of Crystallinity)

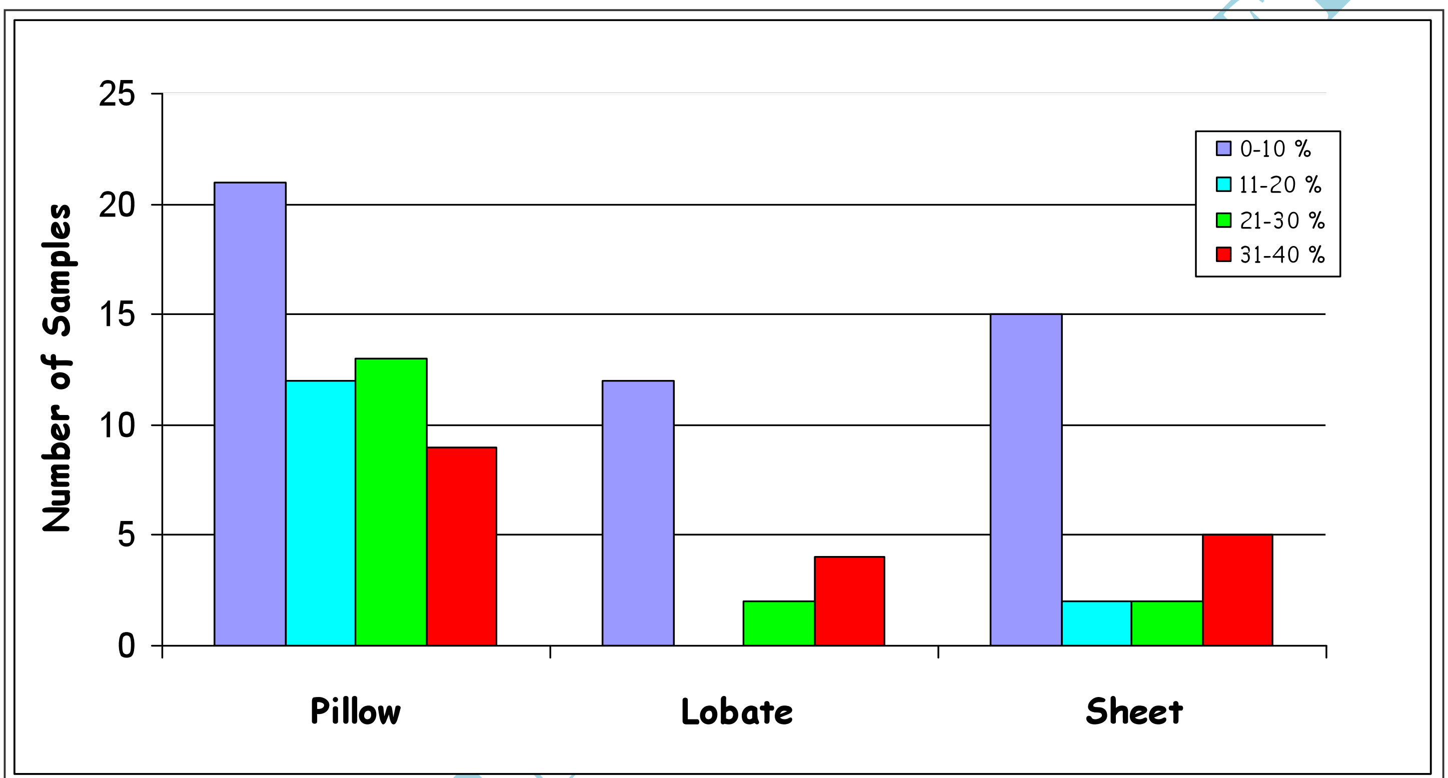

Figure 14. Histogram of crystal fractions data based on lava morphology.

D.) Viscosity Determination

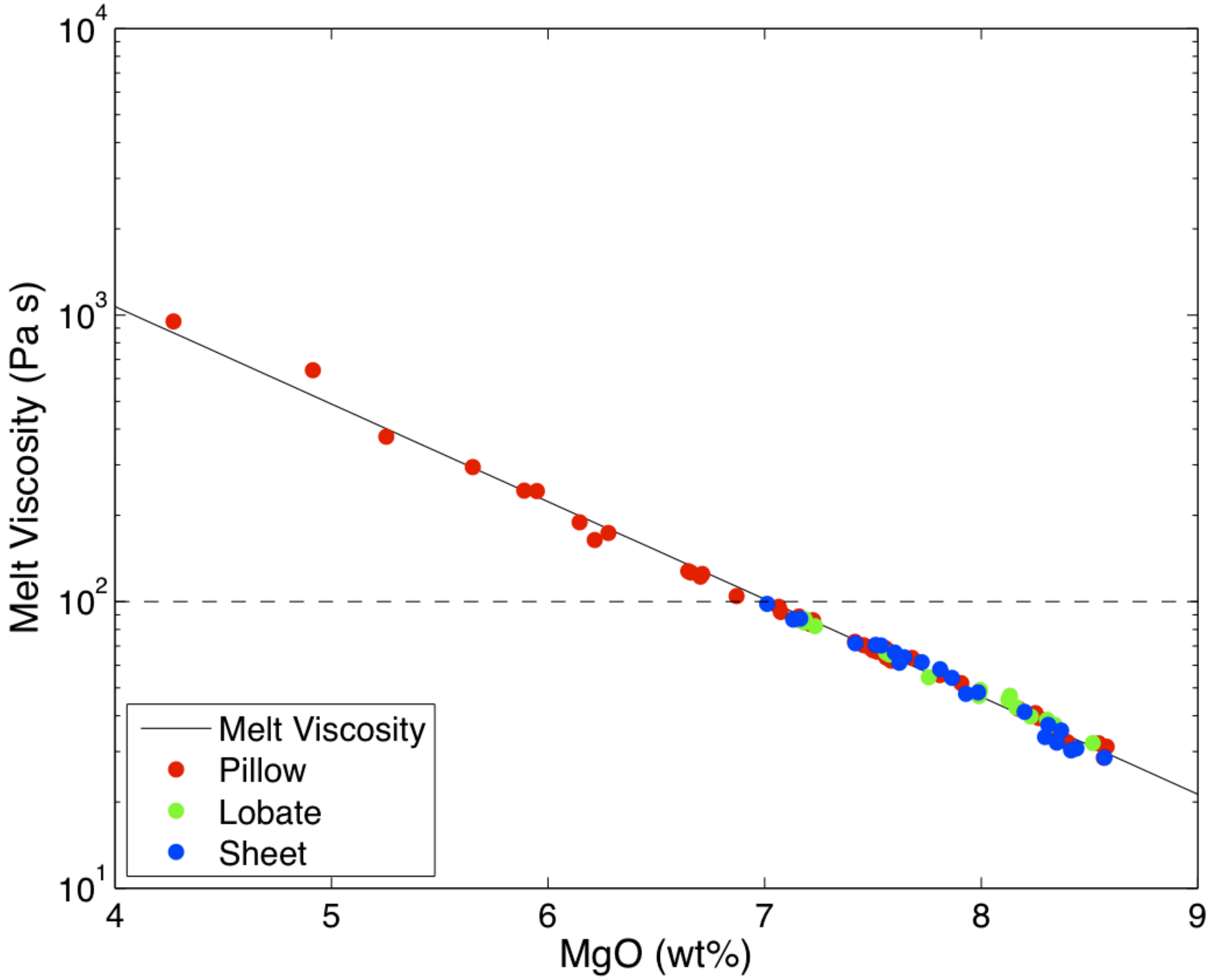

Figure 15. Scatter plot of MgO percentage and melt viscosity plotted on a logarithmic scale. Solid line is a best-fit curve of the data.

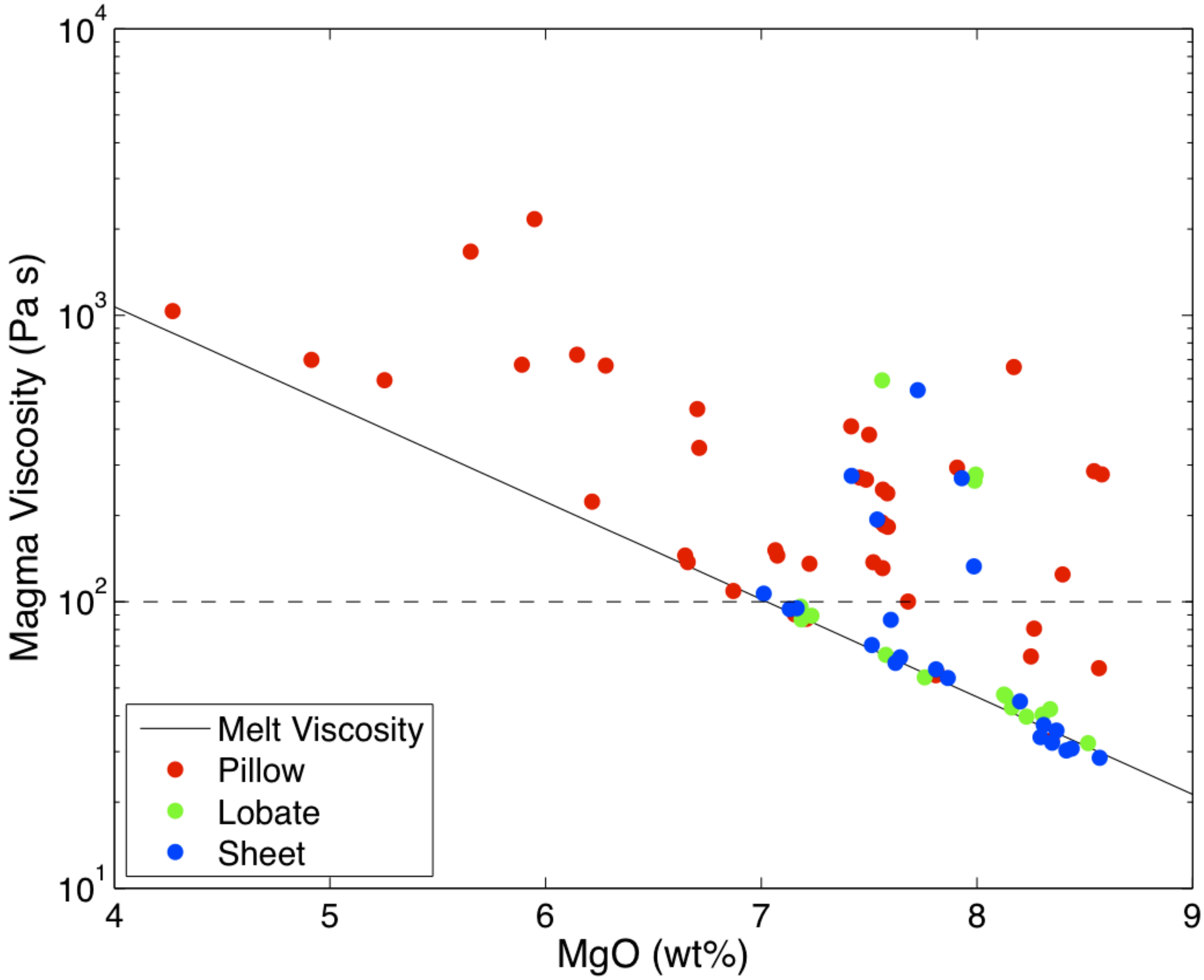

Figure 16. Scatter plot of MgO percentage and magma viscosity plotted on a logarithmic scale. Solid line is the same best-fit curve of the melt viscosity and MgO data plotted in Figure 15.

DISCUSSION

These data show that pillow lavas of the Alarcon Rise are crystal-rich, and that the crystallinity varies greatly, with fractions ranging from 0-40% (Figure 14). Lobates and sheets are composed of lower percentages of crystals, with less variation in percentage composition. Melt viscosities of greater than 100 Pa s, generated only pillow lavas (Figure 15).

Figure 16 shows the same best-fit curve that was plotted in the melt viscosity scatter plot, but the melts now incorporate crystal fraction data. The samples that consist of low percentages of crystals have remained on the line of best fit as they were depicted in Figure 15. The samples that consist of higher percentages of phenocrysts have larger magma viscosities compared to their melt viscosities. Over 77% of the pillow lavas have viscosities greater than 10 Pa s, while only ~25% of the lobate and sheet flows have viscosities that exceed this level. The data in Figure 16 show that the magma viscosity increases with increasing crystallinity.

CONCLUSIONS/RECOMMENDATIONS

Preliminary analyses from this study show that

- The presence of phenocrysts (crystals) in the Alarcon rock samples correlated to an increase in the viscosity of the magma that formed the rock.
- Pillow flow samples contained a high concentration of crystals, and were also highly viscous in contrast to both and sheets and lobates.

In conclusion, our data show that crystallinity and resultant magma viscosity play an important role in dictating the morphology of basaltic lava that is formed on the neovolcanic zone of the Alarcon Rise in the Gulf of California.

Less than one percent of the Earth's mid-ocean ridge system has been thoroughly surveyed, so our understanding of the morphological and geochemical characteristics of mid-ocean ridge systems is still largely unknown. Modern sampling techniques and mapping technologies, such as have been developed at MBARI, are allowing scientists to study submarine volcanism with greater efficiency and proficiency. Studies of the Alarcon Rise contribute greatly to our understanding of the dynamics of sea floor spreading processes, but there is much more work to do.

RECOMMENDATIONS FOR FURTHER STUDY INCLUDE:

- Completing the crystal fraction analysis for the remainder of the rise, and for the off-axis seamounts.
- Quantification of crystal composition analysis, with the use of Photoshop and other tools.
- Completing the mapping the specific flow boundaries using GIS.
- Analysis of trends for viscosity/crystallinity and seafloor morphology from the Tamayo Transform Fault to the Pescadero Tranform Fault (=trends from the southwest to the northeast end of the Rise).
- Comparison of elemental analysis with those of other MOR systems, such as the Juan de Fuca and Mid-Atlantic Ridge systems, as well as the other portions of the East Pacific Rise.

ACKNOWLEDGEMENTS

This summer internship project required the assistance of many people who are affiliated MBARI. I want to wholeheartedly thank David Clague, Julie Martin, Jenny Paduan, and Ryan Portner for their immeasurable help and patience with me as this internship, and associated project evolved. I was so fortunate to work with such an amazing group of researchers. I appreciate all of the learning experiences and assistance that they provided through course of this internship.

I also want to thank David Caress and the Mapping AUV Team for the incredible high-resolution maps that allowed us to view sea floor bathymetry in astounding ways. This study, and so many others, would not have been possible without the incredible maps.

I am also indebted to George Matsumoto and Linda Kuntz for their tireless support and enthusiasm as our excellent Summer Intern Coordinators. In addition, I want to thank the other MBARIans who supported me in so many ways this summer. These individuals and groups include: my fellow summer interns, Judith Connor, The Video Lab personnel, Mariah Salisbury, Dana Lacono, Kim Fulton-Bennett, The Surfing Squirrels, Brian Dreyer, Charles Paull, Kurt Buck, John Ryan, The BBQ Czars, and the people who share the Hadal Common Room.

I am also indebted Chris Scholin and the Packard Foundation for creating this amazing internship opportunity at MBARI. Everyone I encountered at MBARI was incredibly supportive of all of the interns, and the Summer Internship Program. Thank you all!

REFERENCES

Clague DA, and Paduan JB. 2008. Submarine basaltic volcanism, *in* Submarine Volcanism and Mineralization: Modern Through Ancient, (eds) B. Cousens and S. Piercey. Geological Association of Canada, Short Course 29-30 May 2008, Quebec City, Canada.

Compton RR. 1962. Charts for estimating percentage of composition of rocks and sediments. Appendix 3 *in* Manual of Field Geology. Wiley & Sons, NY, pages 332-333.

(Fink and Griffiths 1992)

Giordano D, Russell JK, and Dingwell DB. 2008. Viscosity of magmatic liquids: a model. EPSL, Accepted 3/08.

Gregg TKP and Fink JH. 1995. Quantification of submarine lava-flow morphology through analog experiments. *Geology*. 23:73-76.

Harris AJL, Dehn J, and Calvari S. 2007. Lava effusion rate definition and measurement: a review. *Bulletin of Volcanology*, 70:1-22.

McPhie, J., Doyle, M. and Allen, R., 1993. Volcanic textures; a guide to the interpretation of textures in volcanic rocks. University of Tasmania, Centre for Ore Deposit and Exploration Studies, Launceston, TAS, Australia (AUS), 196 pp.

Perfit MR and Chadwick, Jr WW. 1998. Magmatism at mid-ocean ridges: constraints from volcanological and geochemical investigations, *in* Faulting and Magmatism at Mid-Ocean Ridges. American Geophysical Union, Geophysical Monograph 106.

Author? Year? Physical Properties of Magma, *in* the Encyclopedia of Volcanoes, pages 181-185.